AGU PUBLICATIONS

Geochemistry, Geophysics, Geosystems

RESEARCH ARTICLE

10.1002/2016GC006378

Acquisition of detrital magnetization in four turbidites

Cyrielle Tanty[1], Jean-Pierre Valet[1], Julie Carlut[1], Franck Bassinot[2], and Sébastien Zaragosi[3]

[1]Institut de Physique du Globe de Paris, Université Paris Diderot, Sorbonne Paris Cité, UMR 7154 CNRS, Paris, France, [2]Laboratoire des Sciences du Climat et de l'Environnement (CEA-CNRS-UVSQ), Domaine du CNRS, Avenue de la Terrasse, Gif-sur-Yvette, France, [3]Département de Géologie et Océanographie, Université Bordeaux I, UMR 5805 EPOC, Talence Cedex, France

Key Points:
- Turbidites are a natural laboratory to study depositional remanent magnetization
- Magnetic alignment obeys a simple scaling law linked to the size of the event
- Turbulence has a direct influence on the magnetic torque, hence on paleomagnetic records of directions

Supporting Information:
- Supporting Information S1
- Figure S1
- Figure S2
- Figure S3
- Figure S4

Correspondence to:
J.-P. Valet,
valet@ipgp.fr

Citation:
Tanty, C., J.-P. Valet, J. Carlut, F. Bassinot, and S. Zaragosi (2016), Acquisition of detrital magnetization in four turbidites, *Geochem. Geophys. Geosyst.*, *17*, 3207–3223, doi:10.1002/2016GC006378.

Received 4 APR 2016
Accepted 18 JUL 2016
Accepted article online 19 JUL 2016
Published online 10 AUG 2016

Abstract Turbiditic events are mostly avoided in paleomagnetic studies and therefore their remanence and magnetic properties are poorly described. Turbidites are exempt of bioturbation and potentially provide pertinent information about depositional remanence. We studied four quaternary turbidites of different origins in marine sediment cores. Upward fining of both magnetic and sedimentary fractions indicates that coarser grains reached the bottom first. We observe a progressive shallowing of the magnetic inclinations between the upper and bottom layers of the turbidites that increases with the size of the events and obeys a simple linear scaling law. Measurements of magnetic anisotropy suggest that hydrodynamic conditions prevailing during deposition seem to be dominant for the alignment of the magnetic grains. We suggest that small spherical grains are randomly oriented with zero resultant magnetization in presence of strong turbulent conditions, while the alignment of elongated grains is constrained by the competition between gravity and magnetic forces. A possible scenario is that under turbulent conditions they tend to rest at the bottom with their long axes parallel to the sediment surface and therefore with shallow inclinations, whereas weakly turbulent conditions like during the smallest (26 cm thick) event do not disturb the magnetic alignment and therefore do not generate inclination shallowing.

1. Introduction

In spite of many significant contributions brought up by paleomagnetic records from sediments, we still have limited knowledge of the processes controlling the alignment of magnetic grains by the ambient magnetic field and their natural remanent magnetization [*Tauxe*, 1993; *Valet et al*., 2014]. This poor understanding has direct consequences regarding the resolution, accuracy, and time constants inherent to the paleomagnetic records.

Experimental studies of artificial sedimentation in laboratory have been attempted for many years with the hope of evaluating the role played by distinct parameters on the timing and degree of alignment of the magnetic grains at different depths within the sediment. One can mention experimental studies concerning the effects of compaction, water content, magnetic concentrations, salinity, carbonate and clay content, flocculation, and many other parameters [*Quidelleur et al*., 1995; *Katari et al*., 2000; *Carter-Stiglitz et al*., 2006; *Heslop et al*., 2006; *Tauxe et al*., 2006; *Shcherbakov and Sycheva*, 2010; *Spassov and Valet*, 2012]. These experiments are very useful and they would provide valuable analog of natural depositional processes if they did not fail to duplicate the depositional conditions of natural sediments due to their very different time scales. It is evidently impossible to conduct laboratory experiments over a very long-time period and therefore to reproduce the calm depositional processes of marine and even lacustrine sediments with typical accumulation rates that rarely exceed a few tens of centimeters per thousand years. Redeposition of natural or artificial sediments in a known laboratory field involves a relatively large density of particles which fall across several centimeters or at most a few meters of water depth. Deposition does not last more than a few days and the experiments fail to duplicate subsequent processes (e.g., bioturbation, progressive compaction, diagenesis) that occur over a long-time period in deep-sea sediments.

Redeposition experiments in laboratory can be compared to fast discharges of natural sediments. Such rapid accumulations of sediments are common in nature and identified as turbiditic events. Turbidites are sedimentary reworking caused by either tsunami, earthquakes, slope instabilities, volcanic processes, large

discharges of materials or other catastrophic events. The main difference between laboratory and natural processes may be the fact that turbidites can be sheared by currents whereas most laboratory experiments are mass-wasting deposits in the absence of currents. Only few experiments have been conducted in flumes [*Griffiths et al*., 1960; *Rees*, 1961]. Turbidites have been subjected to studies dealing with the geometry of the deposits [*Dade and Huppert*, 1994; *Peakall et al*., 2000; *Kneller et al*., 2003; *Peakall and Sumner*, 2015] and with the history and the dynamics of turbidity flows [*Bowen et al*., 1984; *Middleton*, 1993; *Cita et al*., 1996; *Normark et al*., 2002]. Depending on their origin, they are also studied as indicators of paleoseismicity [*Beck et al*., 2012; *St-Onge et al*., 2012; *Campos et al*., 2013; *Drab et al*., 2015] as well as for their paleoenvironmental interest [*Buckley and Cranston*, 1988; *Stoner et al*., 1996; *Toucanne et al*., 2012; *Bourget et al*., 2013; *Bonneau et al*., 2014; *Kǒng et al*., 2016].

Apart a few exceptions [*Kodama and Davi*, 1995; *Dickinson and Butler*, 1998; *Tan and Kodama*, 1998; *Enkin et al*., 2001; *Kim and Kodama*, 2004; *Piguet et al*, 2000], turbidites have been ruled out from paleomagnetic records, as they represent geologically instantaneous deposits. In a recent investigation of upper Eocene-lower Oligocene weakly deformed turbidites exposed in Haute-Savoie (France), the authors [*Piguet et al*., 2000] mentioned that a suitable characteristic remanence was preserved and likely acquired early after deposition in levels that contain magnetite. In this case, magnetization was acquired through early postdepositional reorientation of the magnetic grains and therefore erased previous misorientations resulting from the high level of turbulence governing the depositional processes of turbidites, yet to our knowledge this last point was never properly addressed. The magnetic fabric of a few specific turbidites was also recently investigated from two cores taken from the closed marine basins of the Sea of Marmara and Gulf of Corinth [*Campos et al*., 2013]. The purpose of the study was to discern hemipelagites from "turbidite-homogenites," the hemipelagic interval indicating the time elapsed between the successive earthquakes that generated the turbidite. The results revealed differences in magnetic foliation between the different units which led the authors to propose that this approach can be useful for identifying the stratigraphic intervals of hemipelagic deposits.

Certain conditions, like channeled turbidity currents, are characterized by levees of sediment that generate resuspension of a large amount of material that is subsequently redeposited. Because of the fast character of deposition, there is no time for significant bioturbation. This analogy with laboratory deposition experiments is likely to provide additional information about processes involved in the acquisition of magnetization. In addition sedimentary sequences offer the opportunity of comparing the magnetization of turbiditic levels with the underlying and the overlying hemipelagic sediments.

The aim of the present study is to investigate the remanent magnetization and the magnetic signals of four selected turbidites with different characteristics (carbonate against terrigeneous material, proximal and coarse turbidites against distal, and fine turbidites) compositions and thickness and compare them with the surrounding hemipelagic levels.

2. Core Locations and Samplings

Core MD12-3418 (8.52 m long) was collected by the R/V Marion-Dufresne during the MONOPOL cruise in 2012 in the Bay of Bengal (16°30.27 N; 87°47.92 E) at 2547 m water depth (Figure 1). The alluvial fan of the Gulf of Bengal was formed by major accumulation of sediment from erosion of Himalayas and Tibetan plateau. It is the largest submarine fan in the world with about 3000 km length, 1000 km width, and 16.5 km maximum thickness. It is mainly supplied by the confluent Ganges and Brahmaputra Rivers. The fan area is covered by a large number of channels shaped by turbidity currents [*Curray et al*., 2003; *Curray*, 2014]. Core MD12-3418 was taken in one of the levees along the major channel in the North of Gulf of Bengal (Figure 1) which is an active channel system with thick Holocene levees (about 40 m). The sediment selected for the present study was sampled between 50 and 350 cm below the core top. The hemipelagic sediment is composed of homogeneous dark olive gray mud with locally flat or ondulated darker silty lamines that are easily visible. The levels of the spill-over turbidite are located between 150 and 206 cm.

Core MD01-2477 (38°.133 N; 22°.333 E; 867 m water depth; core length: 20.08 m) was taken during a R/V Marion-Dufresne cruise (October 2001) in the central part of the 115 km long, maximum 30 km wide, and 900 m depth, semienclosed, marine basin that defines the Gulf of Corinth (Figure 1) on the Pagalos fault (vertical fault slip rate around 1 mm/yr) [*Moretti et al*., 2004]. The Gulf of Corinth repeatedly alternated

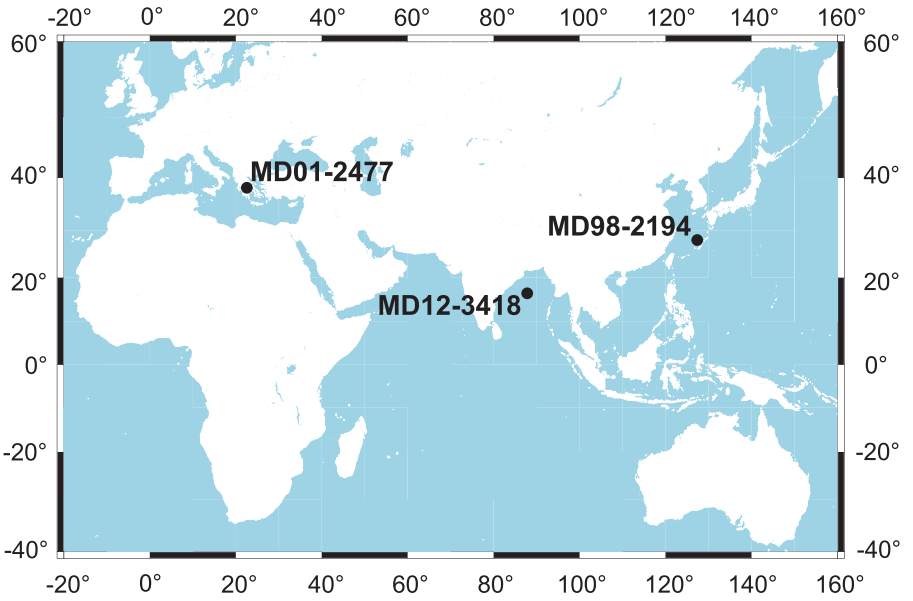

Figure 1. (a) Site locations of cores MD01-2477 (Gulf of Corinth), MD12-3418 (Bay of Bengal), and MD98-2194 (China Sea).

between a lacustrine and a marine basin during the Late Pleistocene due to sea level fluctuations and shallow depth of the Rion-Antirion strait that separates the gulf from Ionian Sea to the west [*Lykousis et al*., 2007]. The A and B marine sections [*Campos et al*., 2013] studied here are located 620–700 cm and 1040–1120 cm above the last lacustrine-marine transition, respectively. The marine sediments (Holocene age) are carbonate dominated sandy/silty turbidites interbedded within homogeneous hemipelagic calcareous mud strata organically rich [*Moretti et al*., 2004]. The turbidites are overlaid by an homogenous layer of fine-grained "homogenites" that represents the upper component of the sequence [*Beck et al*., 2007; *Campos et al*., 2013]. Homogenites are interpreted as long lasting clouds of fine particles that are slowly deposited but their exact nature and limits are not well constrained [*Campos et al*., 2013]. These sequences are related to episodes of higher fluvial input into the gulf that are expressed by sandy beds interpreted as distal turbidites. Slope instabilities could also be responsible for debris flows [*Moretti et al*., 2004]. The two selected "homogenites-turbidites" from this core were previously investigated by *Campos et al*. [2013]. The first 26 cm thick event was found between 663 and 689 cm, while the second 76 cm thick one was sampled between 1041 and 1117cm. The basal layer of both turbidites is easily visible.

Core MD98-2194 (28°06′ N; 127°22′ E; 989 m water depth; core length: 29.8 m) was collected during IPHIS-II cruise (IMAGES IV) of the French R/V Marion Dufresne in 1998. The coring site is located in the Okinawa trough, on the oriental part of Eastern China Sea (Figure 1). Sediment is a clay-rich, hemipelagic ooze, fairly homogenous in color with several 10–170 cm thick ash layers and sandy to silty turbidites which correspond to well-defined intervals of high P wave velocity. A detailed paleomagnetic study including directional, mineralogical, and paleointensity measurements was conducted on the entire core [*Valet et al*., 2011] with the exception of the 174 cm thick turbidite from 9.34 to 11.08 m which was likely caused by a large-scale flank collapse event.

All four turbidites under study were associated with different environmental conditions. They have different thickness of 26 cm, 56 cm (MD12-3418), and 76 cm (MD012477) and 174 cm (MD98-2194).

Sampling was performed using 8 cc transparent paleomagnetic plastic cubes that were gently pushed into the sediment. The mean magnetization level of the cubes is lower than 10^{11} A/m^2 and therefore did not affect measurements of natural remanent magnetization (NRM).

3. Magnetic Mineralogy

We checked for the uniformity of magnetic mineralogy within each stratigraphic sequence by referring to the S ratio defined as $S = 1/2\ [1 - (IRM_{-0,3T}/SIRM_{1T})]$ [*Bloemendal et al*., 1992] which represents the ratio

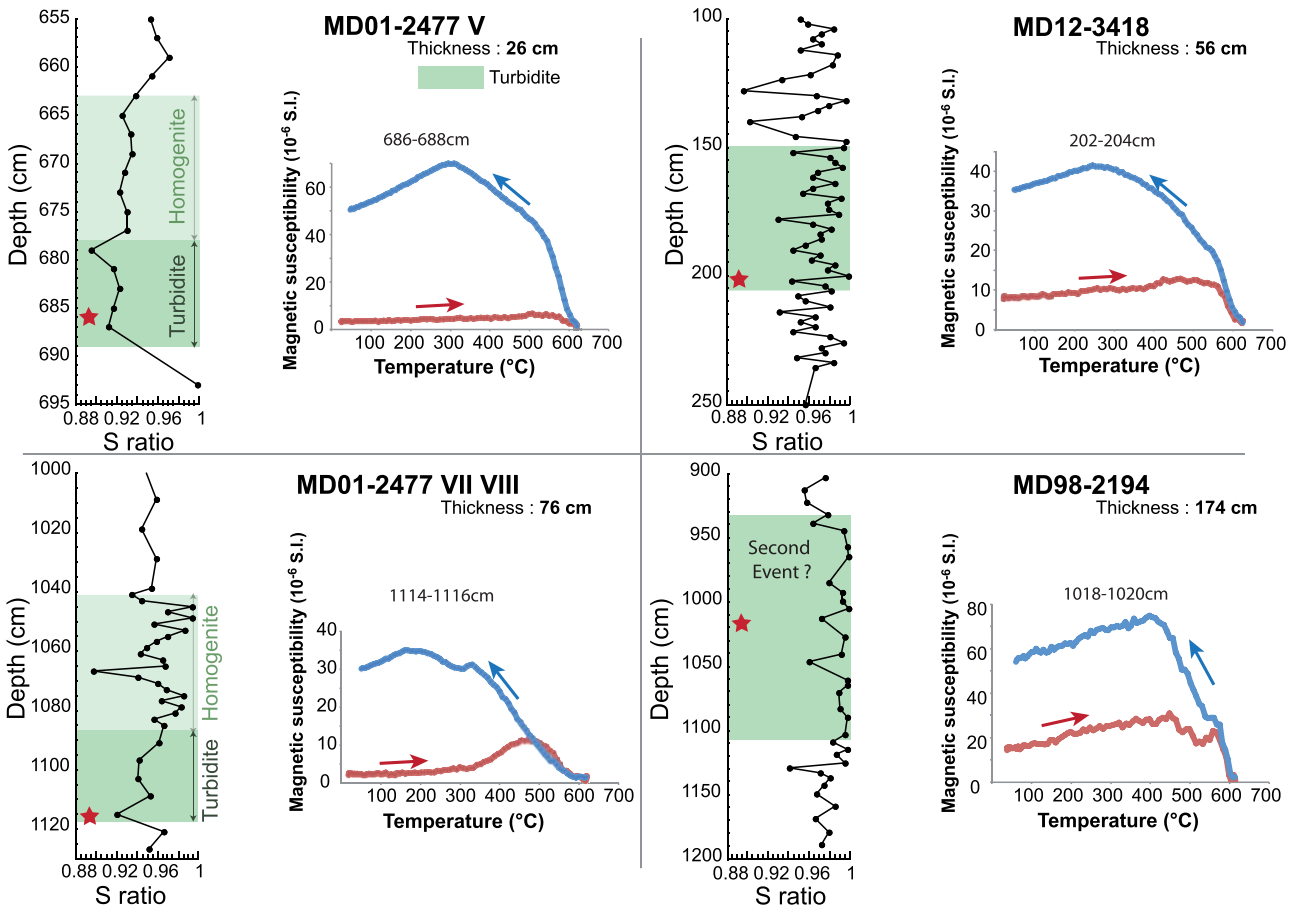

Figure 2. Evolution of magnetic mineralogy within the turbidites. (a) S ratio (red stars correspond to samples used for high temperature measurements) and (b) thermomagnetic curves of magnetic susceptibility versus temperature (heating (cooling, resp.) in red (blue, resp.).

between low and high coercivity minerals. The S ratio was measured using a JR-6 spinner magnetometer after remagnetizing the samples in a 1 T field (SIRM) and subsequently in a 0.3 T (IRM) reversed field using an electromagnet. The S-ratio (Figure 2) does not exhibit significant changes across each sequence. The mean values range from 0.93 for MD01-24177 V to 0.96 for both intermediate size turbidites up to 0.99 for MD98-2194, and indicate that magnetization is mostly carried by low coercivity material, most likely magnetite. High coercivity components (probably goethite and/or maybe also hematite) when present have very little contribution on magnetization.

Low-field thermomagnetic susceptibility (K(T)) measurements were performed at high temperature on 1 cm^3 powders that were crushed from two samples located at the bottom and at the top of each turbidite, using an Agico KLY-3 equipped with a CS-3 (high-temperature furnace apparatus). The CS-3 was used for continuous measurements in air from room temperature up to 600°C.

The results of the thermomagnetic experiments (Figure 2) are consistent with the values of the S-ratio. All heating curves show a major Curie point at 570°C–580°C that is typical of magnetite. Production of magnetite might also result from a few mineralogical changes during heating as evidenced by a slow increase of K before 400°C which could be caused by oxidation of sulfides and large susceptibility values during cooling in core MD01-2477. There is no indication for the presence of greigite in the absence of large transformation above 300–350°C. The sediment from MD98-2194 is characterized by a decrease of susceptibility beyond 450°C that continues after a presumed Hopkinson peak at 550°C. A first phase with a Curie temperature of about 560°C is likely associated with titanomagnetite with little amount of titanium, while a second phase is pure magnetite. Samples from levels located outside the turbidite have a more complex pattern

with a drop of K at 300°C that could either reflect loss of substituted magnetite beyond its Curie point and/or conversion of pyrrhotite into magnetite. This difference may be indicative of different sediment sources for the turbidite and for the hemipelagic layers.

In summary, both magnetic mineralogy and grain density are relatively constant and cannot generate first-order changes in the downcore evolution of the rock magnetic parameters.

4. Grain Sizes Studies

4.1. Bulk Sediment

Turbidites are frequently identified in sedimentary sequences from large changes of sediment grain sizes. Grain-size analyses were conducted on samples from core MD98-2194 with a laser diffraction microgranulometer MALVERN™ Mastersizer 2000 at the GEOPS laboratory (Paris XI-Orsay University). Among different classical statistic parameters, we selected the median D_{50}, expressed in μm, to characterize the grain-size evolution across the different layers. Grain-size measurements of sediment from core MD01-2477 [*Campos et al*., 2013] and core MD12-3418 were both performed using a Malvern Mastersizer Granulometer.

In Figure 3a, we show the evolution of grain sizes as a function of depth in the four sections, in addition, SEM observations are displayed in Figure 3b. The sequences were ordered with respect to the thickness of the turbidites. In all cases, the median grain-size profiles display a significant upward fining confirmed by bulk SEM data. The thickness and the amplitude of the signal marking coarse grain intervals are different in each turbidite, but their overall profile is similar. Note also that the bases of the two turbidites from core MD01-2477 are characterized by a singular large and sharp grain size increase at the bottom of the turbidite that is not present in the other two cores. Except for these two peaks, the mean grain size is not strikingly different between all cores (between 20 and 40 μm).

Core MD98-2194 displays a specific behavior with a progressively thinning-upward grain size from about 1000–1110 cm that is immediately followed by a second coarsening. This evolution may indicate two successive events. Assuming the likely hypothesis of a seismic event, this second anomaly could have been generated by a large aftershock.

The units located above the turbidite sequences have relatively constant median grain sizes between 8 and 5 μm for MD01-2477 V, 8 and 6 μm for MD12-3418, 15 and 5 μm for MD01-2477 VII & VIII, and between 15 and 5 μm in MD98-2194. Another small turbiditic event is likely indicated by a 26 μm grain size level in core MD98-2194 at 1140 cm depth.

4.2. Magnetic Fraction

We have investigated whether the size of the magnetic particles follows the same evolution. We used the anhysteretic remanence (ARM) to the low-field mass susceptibility (X) ratio to scrutinize the evolution of magnetic grain size as a function of depth in each sequence. This ratio has the advantage of being primarily sensitive to magnetite and thus avoids any bias linked to changes in magnetic mineralogy. Some authors prefer the ARM/SIRM ratio that has also been used here for comparison, but SIRM covers a large range of grain sizes and is also sensitive to changes in magnetic mineralogy.

Acquisition of Anhysteretic Remanent Magnetization (ARM) was performed in a 50 μT steady field and 80 mT AF peak field using a Schönstedt demagnetizer that was equipped for that purpose. The ARM measurements were performed on a 2G cryogenic magnetometer. Low-field mass susceptibility was measured with a CS3-KLY3 instrument after weighting the samples (assuming that residual water content was negligible). The ARM/X and ARM/SIRM ratios depict the relative evolution of magnetic grain sizes with depth, but they cannot be used to determine the range of grain sizes involved in the magnetization. More detailed analyses were conducted on gelcap samples using the IPGP alternating gradient magnetometer (AGFM: Princeton Measurements Corporation). We analyzed the hysteresis and the back-field curves to extract the Mrs, Ms, Hcr, Hc parameters at room temperature. The range of magnetic grain sizes was constrained by the hysteresis parameters [*Day et al*., 1977; *Dunlop*, 2002]. In Figure 4b, the Hcr/Hc versus Mr/Ms ratios show that all samples from the four turbidites fall within the pseudo-single domain (PSD) range [*Dunlop*, 2002] and that all data points from the three smaller events are very well grouped.

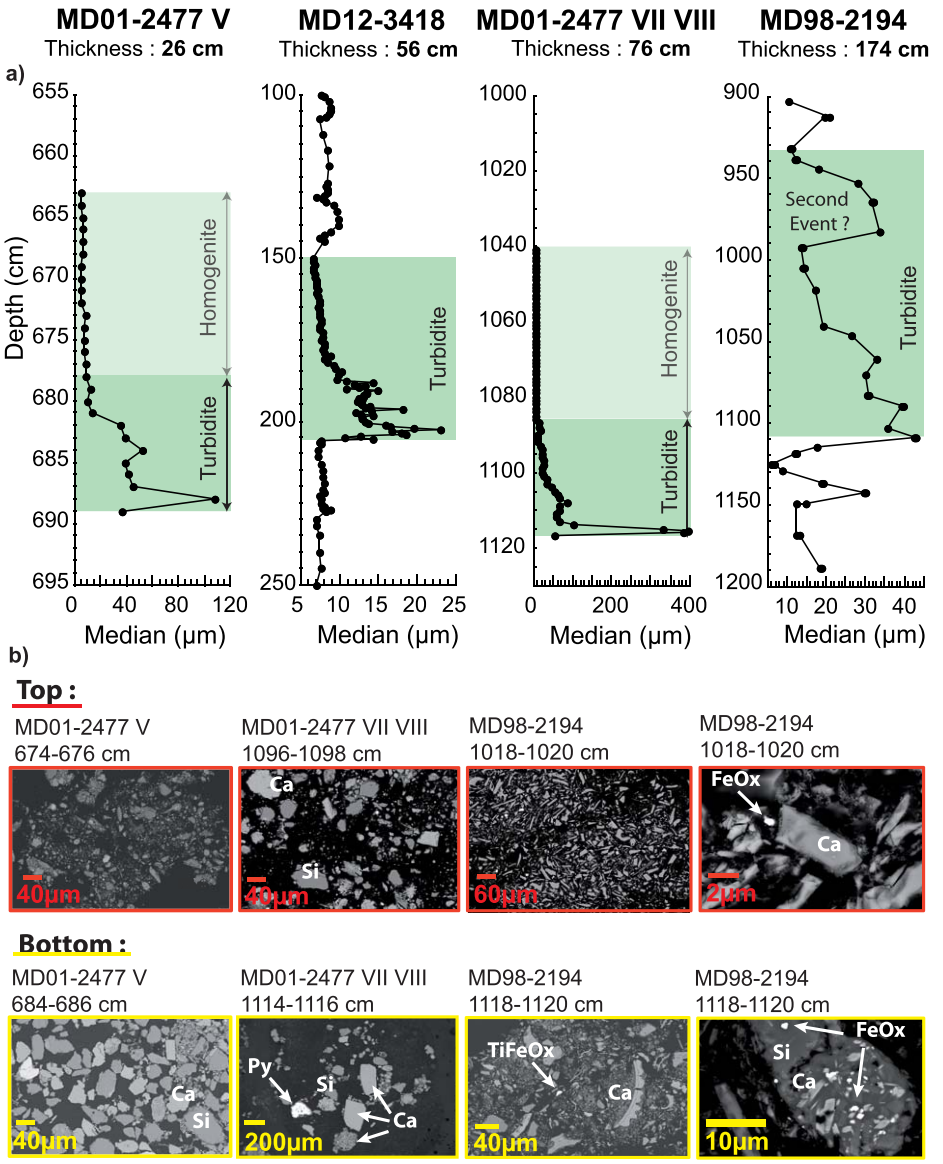

Figure 3. Sedimentary grain sizes (a) as a function of depth (redrawn from *Campos et al.* [2013] for core MD01-2477) (b) SEM images of sediment from top and bottom layers from MD01-2477 V, MD01-2477 VII and VIII, and MD98-2194. Sediment matrix is mostly composed of silica (Si) and calcium/magnesium carbonate (Ca). Coarse titanium-rich iron oxide grains (TiFeOx) and pyrite (Py) are sometimes observed. Iron oxides (FeOx) were only spotted using higher resolution and are shown for MD98-2194.

The evolution of the ARM/X ratio within each sequence is plotted in Figure 4a while ARM/SIRM is given in supporting information Figure S1. Both ratios increase upward within the three largest turbiditic sequences and thus indicate magnetic grain fining upward with ARM/X values two or three times larger in the upper layers of the turbidites.

The results are not so clear for the small 26 cm thick turbidite from core MD01-2477 V that is described by only a few data points. If the points at 683–685 cm are excluded, the ARM/K ratio is unambiguously flat within both the turbidite and the homogenite. In contrast, the hysteresis parameters show a downward coarsening trend, but the turbidite levels are poorly documented. The S ratio is stable within the sequence and therefore the magnetic mineralogy should not change much. If we refer to the ARM/SIRM ratio (supporting information Figure S1), there is some indication for downward coarsening within the turbidite. It is also interesting that the complete turbidite-homogenite sequence has a pattern similar to that of MD01-2477 VII-VIII from the same core. Summarizing all turbidites seem to be characterized by downward

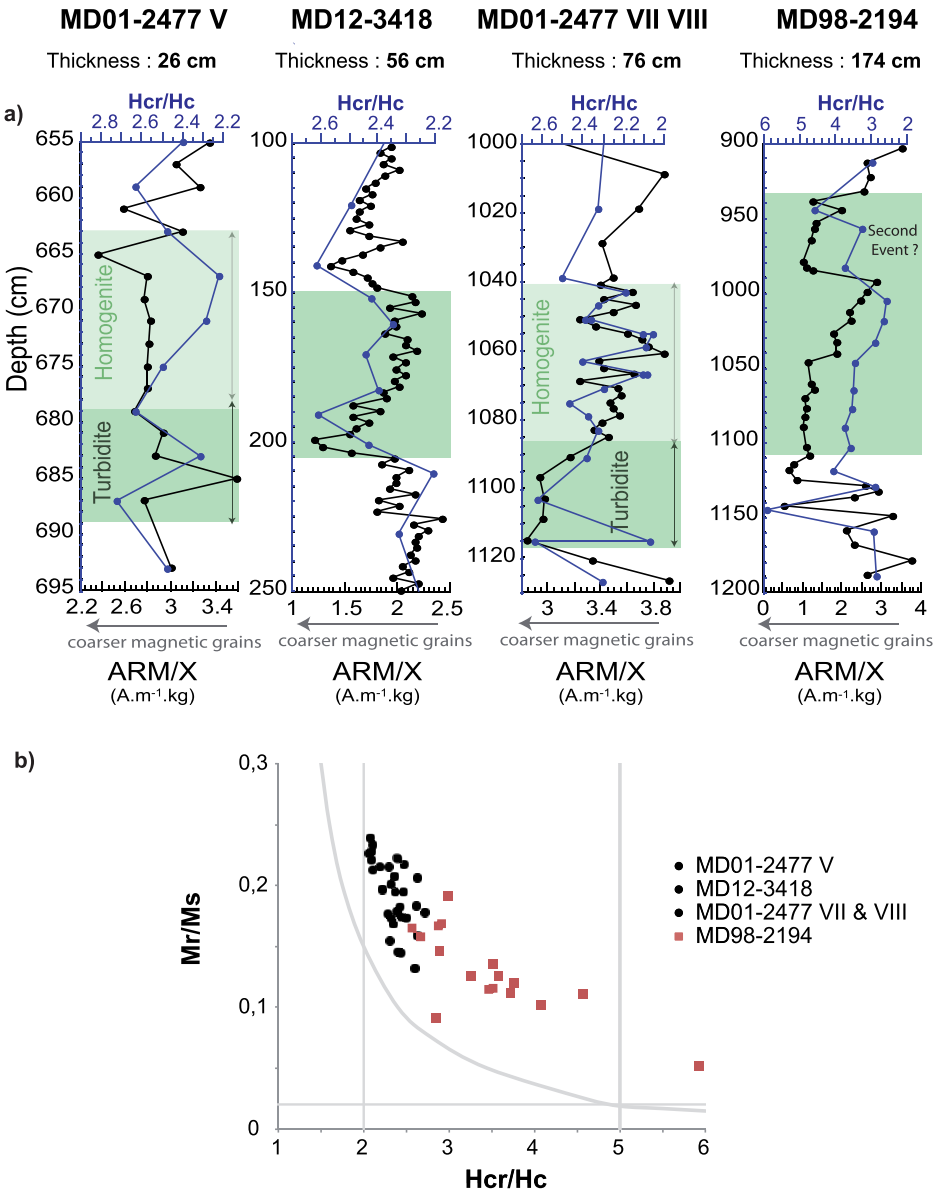

Figure 4. (a) Magnetic grain size. ARM/X (black lines) and Hcr/Hc (blue lines) within the four turbidites as a function of depth. Higher (lower) values indicate smaller (coarser) magnetic grain sizes. (b) Hysteresis parameters (MD01-2477 V, MD12-3418, and MD01-2477 VII and VIII (black dots) and MD98-2194 (red squares): Mr, saturation remanence; Ms, saturation magnetization; Hcr, remanent coercivity; Hc, and coercive force).

coarsening of the magnetic grain sizes, similarly to what has been observed for the bulk sediment grain sizes. The amplitude of this pattern increases with the size of the event. We also mention that the two distinct events derived from the evolution of sediment grain sizes in core MD98-2194 are also reflected by the evolution of the magnetic grain-size. The day plot in Figure 4b also indicates that coarser magnetic grains are present within this large turbidite (red squares in Figure 4b) that could have some influence on the acquisition and stability of the remanence. Whether this is indicative of sediment source or linked to the transport will be discussed below.

5. Inclination Profiles

The Natural Remanent Magnetization (NRM) was measured using a 2G cryogenic magnetometer. All samples were stepwise demagnetized using an AGICO LDA-3 alternating field demagnetizer at 5 mT steps up to

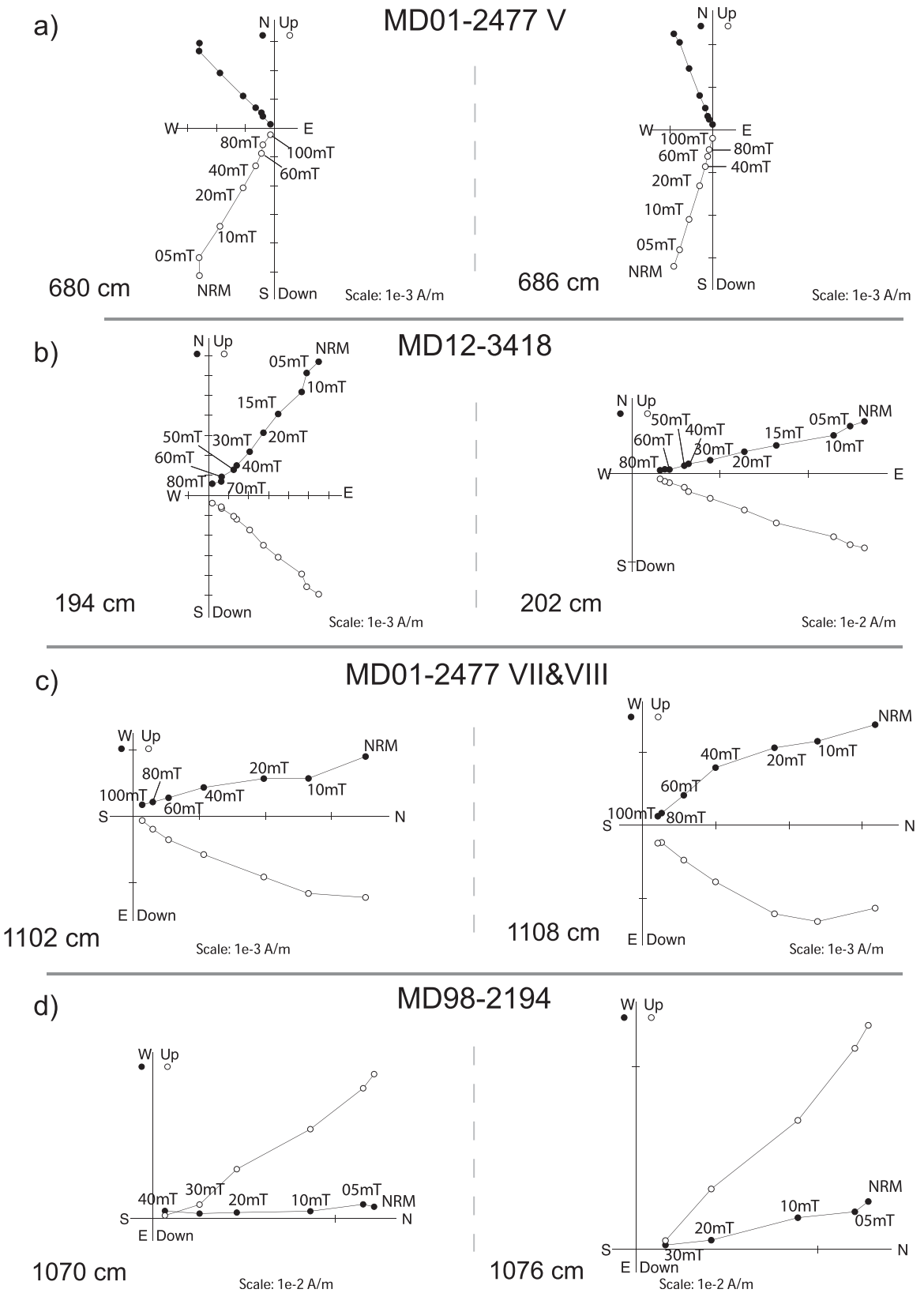

Figure 5. Demagnetization diagrams. Typical vector end-point diagrams for two samples from each turbidite. Solid symbols (open symbols, resp.) correspond to projections onto the horizontal plane (vertical plane, resp.).

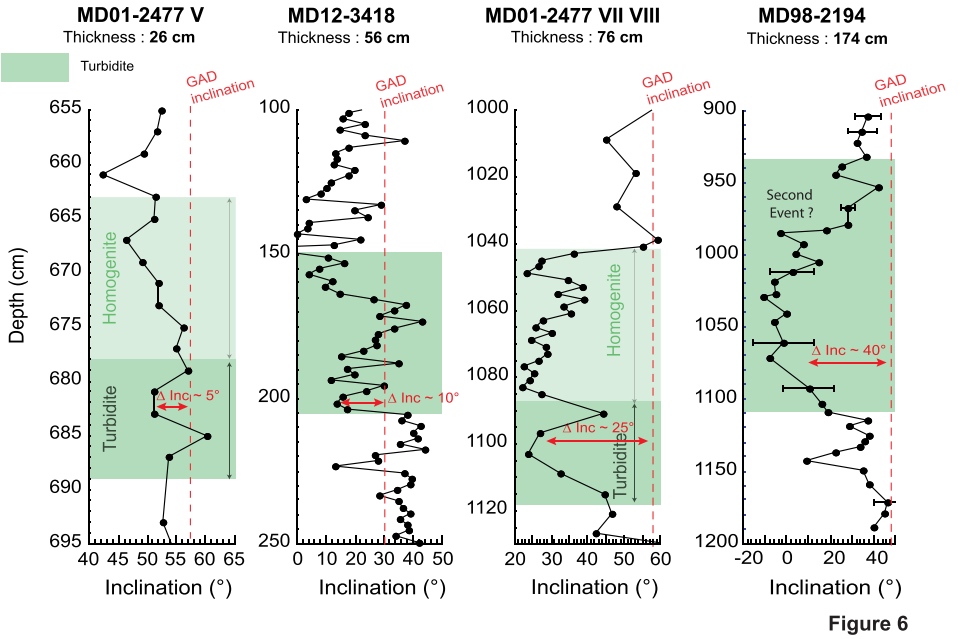

Figure 6. Inclination as a function of depth. The red-dashed lines indicate the inclination of the geocentric axial dipole (GAD) at the site.

30 mT and then by steps of 10 mT up to 80 mT. The characteristic component of magnetization was interpreted by least squares analysis. Typical examples of demagnetization diagrams are shown in Figure 5. Given the young age of the sequences, we only considered diagrams with a well-defined direction passing through the origin of the demagnetization plot. A few diagrams with highly scattered successive directions that prevented to define a characteristic component passing through the origin have been rejected. Samples from the larger turbidite were fully demagnetized after the 40 mT step attesting for lower coercivity of magnetic carriers likely due to larger grains of magnetite.

The cores were not oriented in the horizontal plane and therefore the declination could not be used to test directly for the quality of the magnetic alignment. We took advantage of high-resolution measurements performed in core MD98-2194 to scrutinize the successive declinations after adjusting all values outside the turbiditic layers to 0° mean declination. Declination rotates progressively within the lower 60 cm of the turbidite and then moves back to directions close to 360°. The second presumed event at 980 cm shows a similar pattern. The downcore variations in inclination are shown in Figure 6 for the four turbidites. In each case, we also show the inclination expected at the drilling site (dashed red lines).

In all cores, there is a thin layer at the bottom of the turbidite which does not show any deviation from the expected value, while the overlying levels reveal a deflection that increases with the size of the event. Almost no deviation from the Geocentric Axial Dipole (GAD) value is present in the 26 cm thick small event from core MD01-2477 V, while there is a small offset for the 56 cm event of core MD12-3418 and large deviations by 25° and 40° in the 76 and 174 cm turbidites from cores MD01-2477 and MD98-2194. The inclination approaches the GAD value in the upper part of the turbidites (except in MD12-3418) and meets the expected value in the hemipelagic levels. In the case of the very large event recorded within core MD98-2194, the evolution is progressive from bottom to top. Unlike grain size variations and the declination record, the inclination does not indicate the presence of a second small event in the upper part of the turbidite.

We performed a first set of measurements that revealed shallow and sometimes negative inclinations within the thick turbidite of core MD98-2194. We investigated several possible origins that could have generated this behavior. The demagnetization diagrams (Figure 5) did not reveal any systematic bias so that there was no reason to suspect any artifact. Another possibility was that the magnetic grains were mechanically reoriented during coring. However there are no reasons why reorientation would have been restricted to the lower layers of the turbidite. Density measurements and lithological parameters do not indicate any difference with respect to the other layers. Last, we investigated the role played by magnetic viscosity. A

second set of samples was taken from the working and archive halves of core MD98-2194. Immediately upon returning to the laboratory the NRM was measured, then the samples were placed within a μ-metal box for 6 days before performing a second measurement. The samples were then put in position 1 in the earth's magnetic field (supporting information Figure S2) for 1 week. The NRM was measured at day 13, then the samples were turned upside down in position 2 and measurements were performed again 9, 15, and 21 days later (days 22, 28, and 34 in supporting information Figure S2). The downcore evolution of the inclination (supporting information Figure S2) shows no difference between the first and second measurements. The largest discrepancy occurred at day 13 (position 1). There were no more negative values and after 22, 28, and 34 days (position 2) the evolution was negligible. In light of these results, we assume that the samples between 1065 and 1085 cm carried a short-term magnetic viscosity. Since the first batch of samples was measured after a few days spent in the laboratory, this could explain the initial presence of negative inclinations (supporting information Figure S2). The error bars plotted in Figure 6 represent the deviations between the successive measurements that were performed at the presumably viscous levels.

6. Magnetic Alignment

6.1. Magnetization and Grain Sizes

In the following discussion, we discard the small 26 cm event recorded in core MD01-2477 that does not display any marked evolution of the magnetic parameters. We will later come back to this core.

Both sediment and magnetic grain sizes display a coherent pattern within all turbidite layers with coarser grains in the lower levels. We rescaled each turbidite to a common thickness and we normalized the magnetic grain size indicators to their maximum value to compare them between all sections. The rescaled magnetic grain sizes (Figure 7) are relatively coherent between each sequence. In all cases, magnetic grains stop thinning at a rescaled thickness of about 0.7, but the path to reach this point is different for each event. The pattern appears to be consistent enough to consider that at first-order magnetic size grading seems to be independent from the thickness of the event. The depositional process always seems to generate similar size distribution of particles whatever their concentration.

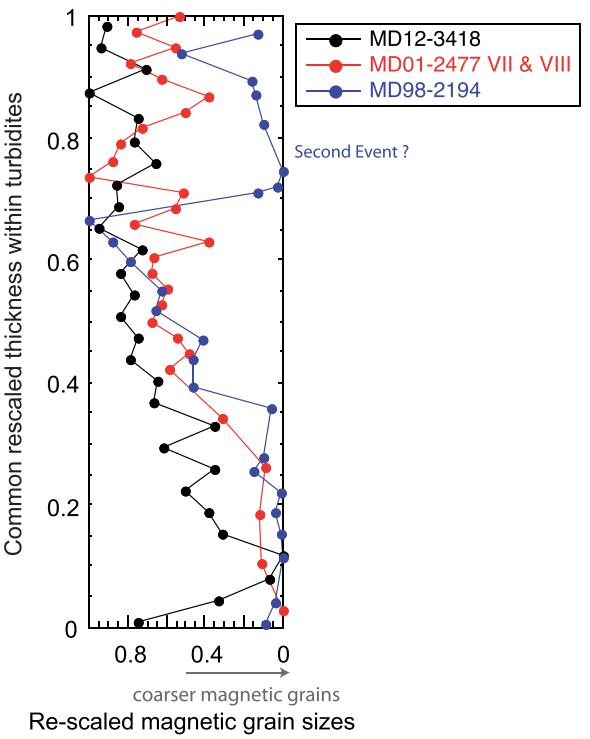

Figure 7. Evolution of the ARM/K ratio as a function of depth. The magnetic grain size indicators (ARM/K) have been normalized to their maximum value and the depths have been rescaled to the same common thickness for all events.

The fact that both the sedimentary and magnetic granulometries have similar profiles (Figures (3 and 4), and 7) is difficult to reconcile with the concept of magnetic grains embedded within sedimentary particles that are frequently referred as clusters. In that case a whole range of fine to coarse magnetic grains would be associated with coarse sedimentary grains. Assuming that magnetic and sedimentary grains are initially dispersed and separated from each other, they fall independently from each other in water. The fact that both granulometries display the same profile with depth can result from two possibilities. The first one is that the coarser magnetic and the coarser sedimentary grains reached the bottom separately without forming clusters. However, this is unlikely given the density of particle collisions and therefore clusters are likely to be built. Therefore, the second most reasonable scenario is that flocculation was initiated in the water column, but only after segregation of the coarse magnetic and sedimentary grains, thus not in the early stage of discharge. This

scenario implies first that previous clusters of particles break down by frictions within the slurry during accelerated turbulent movement, and then the existence of gravitational sorting by particle size followed by collisions during descent in water with possible formations of new, but sorted, clusters. The SEM observations are compatible with this scenario as clusters of coarse magnetic grains embedded within silicate and carbonate were repeatedly spotted in the bottom part of the turbidites (as in MD98-2194, Figure 3b). Aggregates or clusters were likely not formed after deposition because the very fast accumulation of sediment impeded any postdepositional reorientation or grain motion after they reached the bottom. In contrast, if we were dealing with hemipelagic sediments, low depositional processes would not hamper subsequent rotations or coalescence of grains. In the present situation, the system was immediately locked, making impossible any subsequent reorientation of magnetic grains once they reached the bottom. This is in contrast with the depositional processes associated with usual accumulation rates of hemipelagic sediments that leave the magnetic grains free of being oriented by the field.

Assuming that up-core grain size variation was also accompanied by higher particle density during this early stage of the deposits, we can investigate further whether there is a systematic relationship between the two parameters. In supporting information Figure S3, the sedimentary grain sizes are plotted as a function of the inclination deviation from the (GAD) value at the site. There is no well-defined relationship with inclination, which again supports a decoupling of the sedimentary and magnetic fractions.

If we turn towards magnetic grain sizes, the unique evidence for some relationship is observed for the large event of core MD98-2194. The phase between 1100 and 1050 cm is associated with small ARM/K ratios that are indicative of coarser magnetic grains and that are accompanied by a large deviation of inclination. We mentioned above that the hysteresis parameters (Figure 4b) revealed the presence of coarser grains within this turbidite, which may not be without consequence on the inclination record. However, the correlation is rather weak.

6.2. Anisotropy of Magnetic Susceptibility and Anhysteretic Remanence

Shallower inclinations than expected are frequently observed in sediments [*Tauxe and Kent*, 1984; *Khan et al*., 1988; *Collombat et al*., 1993]. They can be inherent to the depositional processes and/or result from compaction of sediment. Compaction generates flattening of ellipsoidal grains and is thus easily identified by measurements of magnetic anisotropy. The anisotropy of anhysteretic remanence (ARM anisotropy) and the anisotropy of magnetic susceptibility (AMS) are thus helpful to identify and correct for inclination shallowing in natural sediments and/or sedimentary rocks [*Jackson et al*., 1991; *Collombat et al*., 1993; *Tan*, 2003]. The technique has also been applied to laboratory redeposited sediments [*Levi and Banerjee*, 1990; *Kodama*, 1997; *Tan et al*., 2002].

In the present cores, the inclinations are lower than expected by up to 40° (Figure 6) and in the case of core MD98-2194 the deviations reach values that are larger than typically reported in the literature, for example $\Delta I = 20°$ in *Khan et al*. [1988], 25° in *Tauxe and Kent* [1984], 30° in *Collombat et al*. [1993], and 40° in *Garcés et al*. [1996]. In order to investigate a possible link between the orientation of the elongated magnetic grains and the inclination deviations, we measured the AMS of samples distributed within all cores using a KappaBridge KLY-3 susceptibility bridge and the Paleomac software [*Cogné*, 2003]. The foliation increases upward in the sequence, while the lineation is stable. The K_{min} inclination does not show any clear correlation with the percentage of anisotropy (Figure 8). It is characterized by larger amplitude oscillations in core MD98-2194. The tendency is the same for the surrounding layers that are associated with calm depositional processes and therefore precludes any interpretation in terms of depositional conditions. The range of anisotropy does not change much between and within the sequences. The down-core pattern of the degree of anisotropy and K_{min} inclination have no specific trend within the turbidites. From these results, we reasonably consider that the magnetic fabric does not seem to be responsible for any bias in the inclinations.

The lack of direct link (supporting information Figure S4) between **t**he lineations indicated by the AMS and the NRM declinations is not surprising since the AMS is constrained by paramagnetic and ferromagnetic grains (supporting information Figure S4) that are mostly not involved in the remanence. In order to deal with the same grain sizes as those involved in the remanence, we relied on the anhysteretic remanence. The anisotropy of ARM was investigated on samples distributed within the large turbidite (MD98-2194) that has the largest NRM inclination deviation. In Figure 9 we compare the declinations of the Kmax axes with

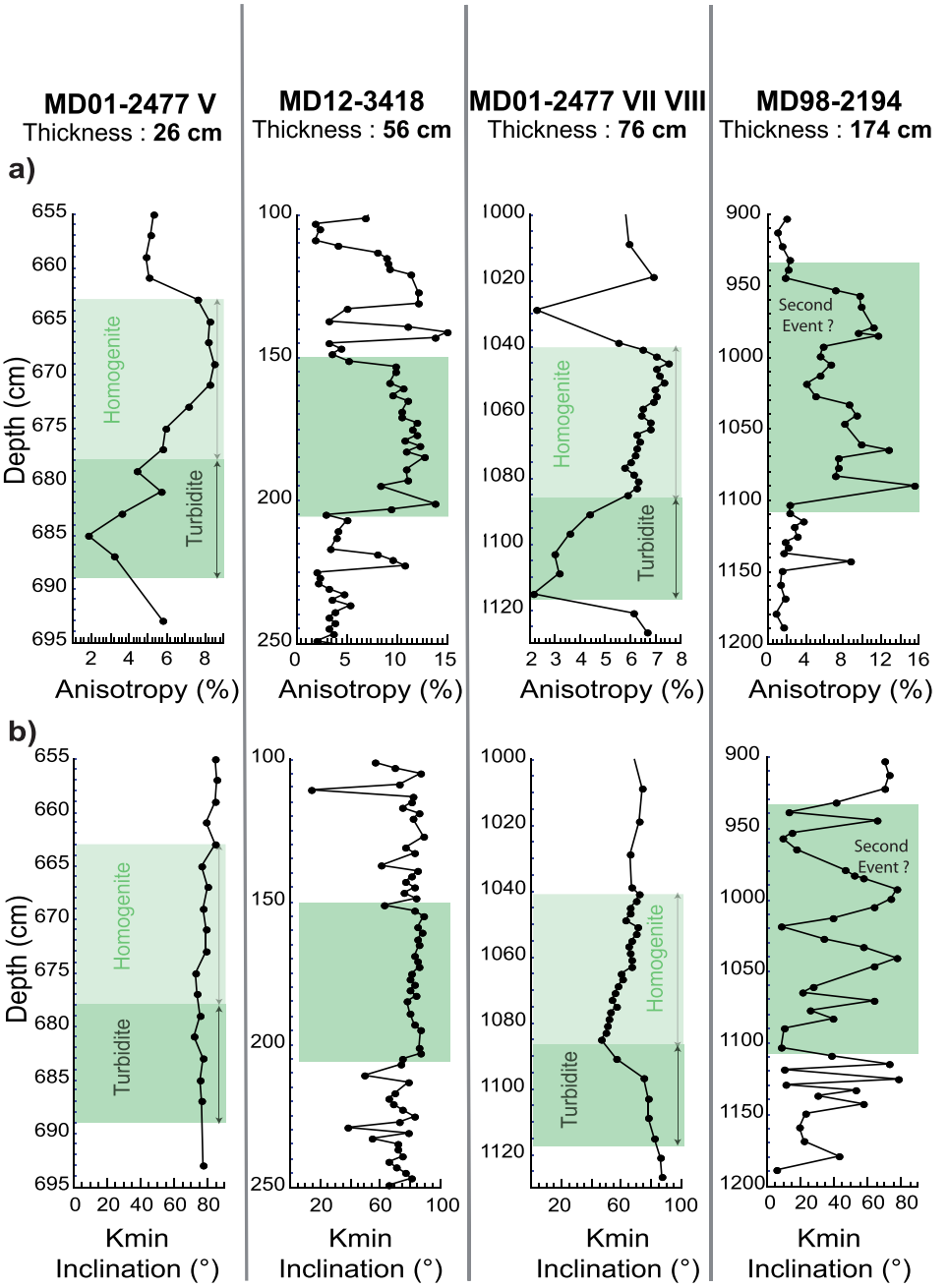

Figure 8. (a) K_{min} inclination and (b) degree of anisotropy of magnetic susceptibility along the four turbidites.

the corresponding declinations of the NRM. As the Kmax axes are defined within a 180° quadrant, directions lying within two opposite sectors are similar. Therefore, the present ARM Kmax axes are found in proximity to the directions (Figure 9) of the remanence. These results suggest that the magnetic field was not the unique factor that governed the alignment of the magnetic grains, but that the orientation of the particles within the horizontal plane was constrained by the direction of their long axes, particularly in presence of turbulent conditions that generate large deviations of the inclination. This scenario implies (i) that the elongated magnetic grains tend to lie with their long axes closer to horizontal (ii) that the hydrodynamic conditions governed the orientation of the long axes, and (iii) that the fast accumulation of sediment locked almost immediately their position with no possible subsequent reorientation.

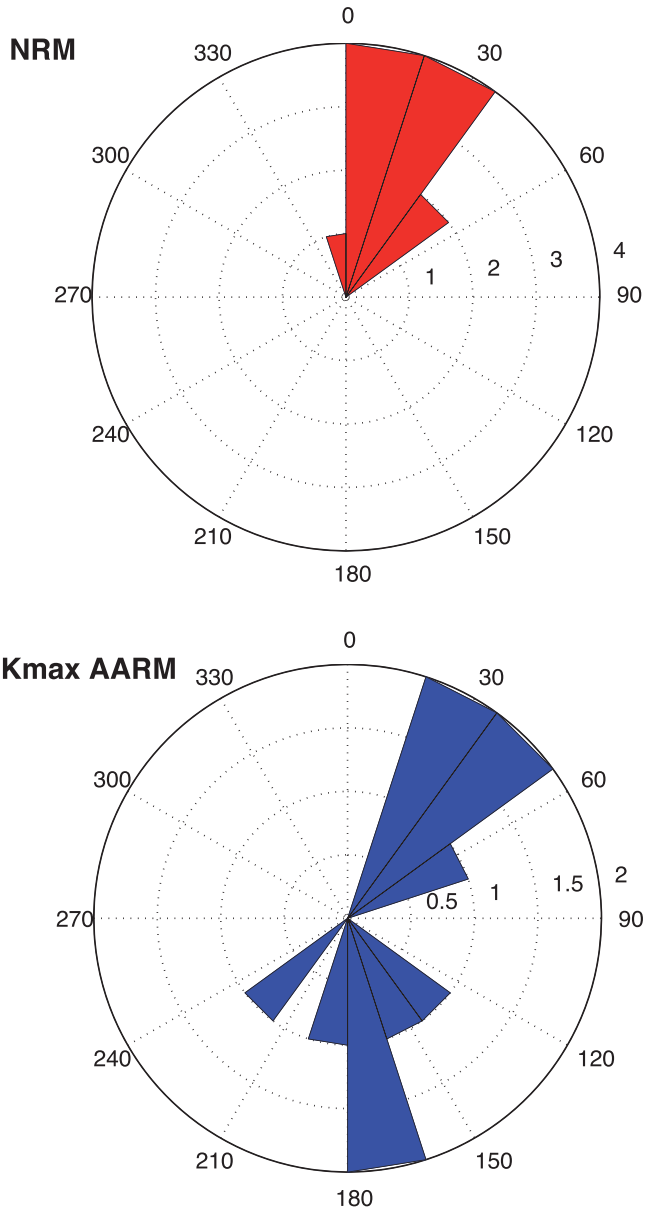

Figure 9. Rose diagrams showing the distributions of the NRM and AARM Kmax axes for MD98-2194.

6.3. Magnetic Alignment

Turbidites are instantaneous events and therefore the upcore variations of NRM/SIRM cannot be linked to any variation of the geomagnetic field, but they provide a first-order estimate of the proportion of low-medium coercivity magnetic grains that have been aligned by the field. We selected the 10 mT demagnetization step for the NRM because the soft components were completely removed at this level. Since the NRM reflects the statistical alignment of the vectors, it can also be seen as an indirect indicator for the quality of alignment. In all events, the mean natural remanent magnetization represents only 0.5% (Figure 10) of the SIRM, which indicates that a very tiny proportion of the grains has been oriented. However, these values do not differ from those that are usually found in natural marine sediments and remain of the same order of magnitude within the hemipelagic layers [*Heslop et al*., 2014].

The mean trend of the NRM_{10mT}/SIRM ratio decreases with depth by a factor 3 within the two larger turbidites (Figure 10) except in the upper part of the large turbidite from core MD98-2194. We discussed above that the corresponding upper levels are likely associated with the occurrence of a second sediment discharge. Therefore, the upper levels do not question the decreasing trend of the ratio over the 1 m thick lower levels. There is only a small evolution of NRM_{10mT}/SIRM in MD12-3418 except for a peak at 200 cm that is accompanied by significant coarsening in grain size and also reflected by larger anisotropy. The same remark holds for the small event of MD01-2477V. We thus infer that the statistical alignment would be related to the size of the events, and thus likely to the flux of particles. In contrast, and despite some variability the two smaller events do not display any trend (unless other factors prevent us to discern an evolution of the ratio).

In order to clarify further a possible relationship with turbidite size, we have represented in Figure 11 the mean-averaged deviation of the inclination with its standard deviation against the size of each event. The results appear to confirm the existence of a correlation between the two parameters, although the low number of data remains a limitation as well as the gap between the size of the large event with respect to the other three. In order to compensate for this gap, we took advantage of the two unique published data of turbidites that include the same parameters (events RL5 and RDL13, in *St.-Onge et al*., [2004]). The results confirm the relationship and are consistent with observations by [*Jezek et al*., 2012; *Bilardello*, 2013] that increased particle interactions increase shallowing.

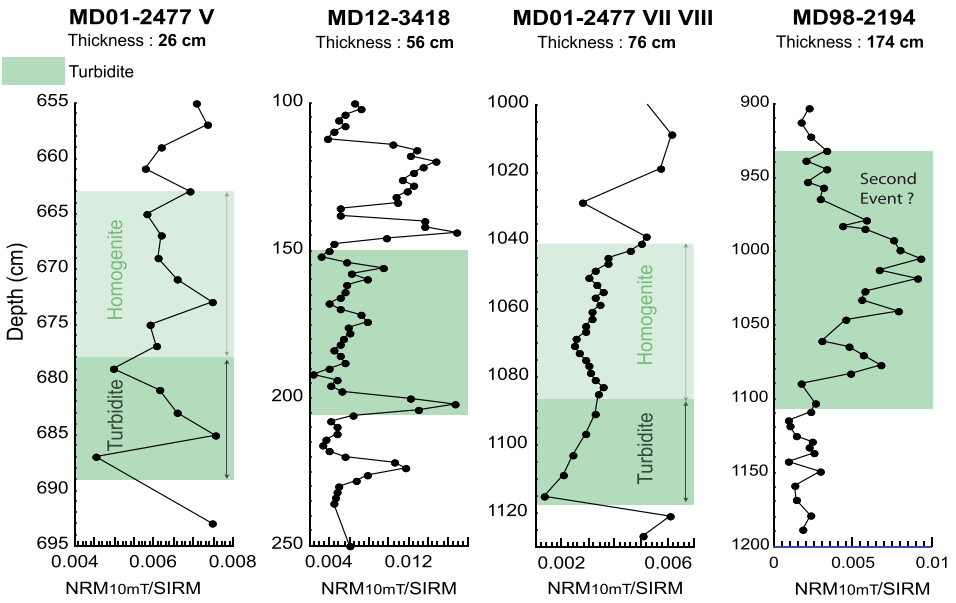

Figure 10. Evolution of the NRM_{10mT}/IRM ratio as a function of depth within the turbidites. This ratio can be seen as an indicator of alignment of the magnetic grains. The 10 mT step of the NRM was selected to avoid any influence of low coercivity secondary component.

From these considerations, we tentatively draw a scenario which emphasizes the role played by turbulence on the acquisition of magnetic remanence and therefore primarily concerns events that involve a large amount of material. In such conditions, the magnetic torque is too weak to counterbalance the effect of the turbulence on the aligment of the particles. The accumulation rate is so fast that this poor alignment remains unchanged once they have settled down.

During the very early stage of the process, a large amount of particles and magnetic grains reach the sediment-water interface. We observed almost perfect alignment within the thin bottom layer of the turbidites. We suspect that partial remobilization of previous deposits followed the first turbiditic arrival. This

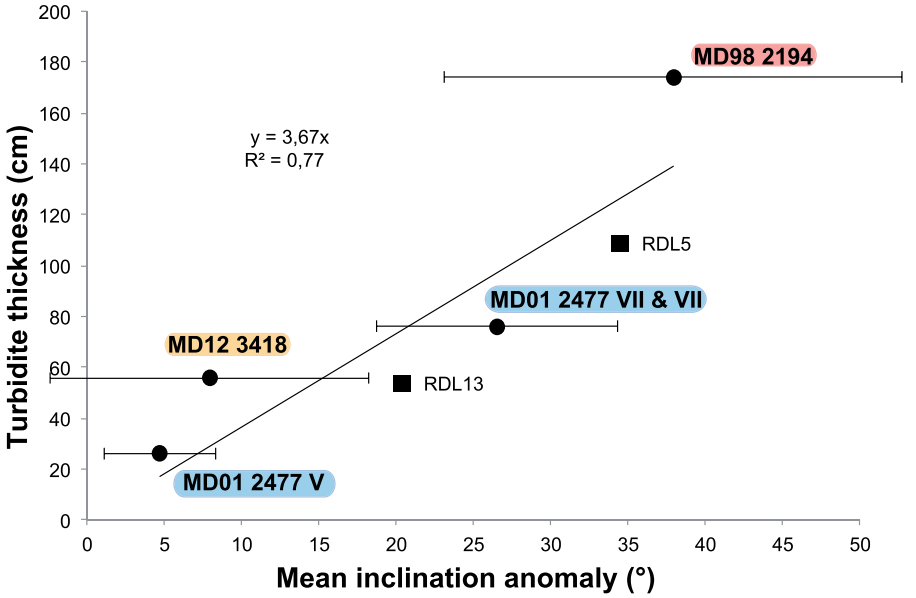

Figure 11. Plot of the linear relationship between the deviation of mean inclination from the GAD value at each site and the turbidite thickness. The compilation incorporates the four turbidites from this study and two additional events (RDL5 and RDL13) from St.-*Onge et al.* [2004].

perturbation generated favorable conditions for partial or complete reorientation of magnetic grains within a very thin layer which was likely the unique layer associated with postdepositional process. This would also explain why this thin bottom layer was not revealed by changes in the sedimentary grain sizes. Immediately above it, large turbulent conditions associated with important discharges generated collisions which contributed to poor orientation of the large magnetic grains. Lower turbulent conditions prevailing during small events might improve the statistical alignment of the grains by the field. We thus assume that deficiency in the alignment of large magnetic grains within big events is primarily caused by enhanced turbulent conditions associated with the early stages of deposition.

These conditions evolved toward quieter depositional regime in the upper layers up to the levels that are associated with calm hemipelagic sedimentation. We have shown that the grain sizes obey a scale law, which suggests that the mechanisms are valid for all events. Therefore, grain distribution always display a similar pattern, the amplitude of turbulence being the main factor driving the deficiency of alignment by the field at the bottom. The scenario is also consistent with the fact that the small turbidite (only 26 cm thick) did not reveal any significant misalignment and that its magnetic characteristics were actually similar to those of the overlying hemipelagic sediment.

7. Conclusions

This study of four turbidites with different sizes and origins reveal several common features which might bear some consequences for processes involved in the magnetization of sediments. In this case, the absence of bioturbation and the very fast accumulation prevents from any reorientation of magnetic grains and thus documents the influence of hydrodynamic conditions prevailing during deposition, especially the role of the turbulence on the acquisition of depositional remanence. This first exhaustive magnetic study of four turbidites has shown that:

1. In all events coarse sediment particles and coarse magnetic grains reach the bottom first, which implies that flocculation was initiated in the water column after segregation of the coarse magnetic and sedimentary grains.
2. The distribution of magnetic grain size with depth satisfies a common scale law for the three larger events.
3. Misalignment of magnetic grains shows no link with anisotropy of magnetic susceptibility, but there is some indication that hydrodynamic forces affect the magnetic orientation of the small grains in presence of strong turbulence.
4. The degree of alignment decreases as a function of the event size. This gives credit to the influence of turbulent conditions and to the amount of particles mobilized at the same time.
5. The small turbidite do not show any large deviation of the directions and therefore reveal similar characteristics as those of the surrounding hemipelagic layers. We infer that these events could be interesting analogues to deposition experiments in laboratory.

An interesting characteristic is that similar processes seem to be operating in all studied cases despite their different origins. We have drawn a simple scenario that emphasizes the importance of turbulence on magnetic alignment.

Acknowledgments
The authors are pleased to ackowledge François Baudin, Edouard Philippe, and Guillaume St-Onge for helpful discussions. Christophe Colin provided technical support and expertise for grain-size analyses at the GEOPS laboratory. Core access was made possible by Eva Moreno. Valery Shcherbakov and two other anonymous reviewers made constructive comments and helpful suggestions that greatly improved the manuscript. The research leading to these results has received funding from the European Research Council under the European Union's Seventh Framework Programme (FP7/2007-2013)/ERC grant agreement GA 339899-EDIFICE. This is IPGP contribution number 3746. All data plotted in the figures are available upon request at carlut@ipgp.fr or valet@ipgp.fr.

References

Beck, C., et al. (2007), Late Quaternary co-seismic sedimentation in the Sea of Marmara's deep basins, *Sediment. Geol.*, *199*(1–2), 65–89, doi:10.1016/j.sedgeo.2005.12.031.

Beck, C., et al. (2012), Identification of deep subaqueous co-seismic scarps through specific coeval sedimentation in Lesser Antilles: Implication for seismic hazard, *Nat. Hazards Earth Syst. Sci.*, *12*(5), 1755–1767, doi:10.5194/nhess-12-1755-2012.

Bilardello, D. (2013), Understanding DRM acquisition of plates and spheres: A first comparative experimental approach, *Geophys. J. Int.*, vol. *206*, 1–11, doi:10.1093/gji/ggt240.

Bloemendal, J., J. W. King, F. R. Hall, and S.-J. Doh (1992), Rock magnetism of Late Neogene and Pleistocene deep-sea sediments: Relationship to sediment source, diagenetic processes, and sediment lithology, *J. Geophys. Res.*, *97*(B4), 4361–4375, doi:10.1029/91JB03068.

Bonneau, L., S. J. Jorry,S. Toucanne, R. S. Jacinto,and L. Emmanuel (2014), Millennial-scale response of a western mediterranean river to late quaternary climate changes: A view from the deep sea, *J. Geol.*, *122*, 687–703, doi:10.1086/677844.

Bourget, J., S. Zaragosi, M. Rodriguez, M. Fournier, T. Garlan, and N. Chamot-rooke (2013), Late quaternary megaturbidites of the Indus Fan: Origin and stratigraphic significance, *Mar. Geol.*, *336*, 10–23, doi:10.1016/j.margeo.2012.11.011.

Bowen, A. J., W. R. Normark,and D. J. W. Piper (1984), Modelling of turbidity currents on Navy Submarine Fan, California Continental Borderland, *Sedimentology*, *31*(2), 169–185, doi:10.1002/9781444304473.ch1.
Buckley, D., and R. Cranston (1988), Early diagenesis in deep sea turbidites: The imprint of paleo-oxidation zones, *Geochim. Cosmochim. Acta*, *52*(12), 2925–2939, doi:10.1016/0016-7037(88)90158-5.
Campos, C., C. Beck, C. Crouzet, F. Demory, A. Van Welden, and K. Eris (2013), Deciphering hemipelagites from homogenites through anisotropy of magnetic susceptibility. Paleoseismic implications (Sea of Marmara and Gulf of Corinth), *Sediment. Geol.*, *292*, 1–14, doi:10.1016/j.sedgeo.2013.03.015.
Carter-Stiglitz, B., J. P. Valet, and M. LeGoff (2006), Constraints on the acquisition of remanent magnetization in fine-grained sediments imposed by redeposition experiments, *Earth Planet. Sci. Lett.*, *245*(1–2), 427–437, doi:10.1016/j.epsl.2006.03.002.
Cita, M. B., A. Camerlenghi, and B. Rimoldi (1996), Deep-sea tsunami deposits in the eastern Mediterranean: New evidence and depositional models, *Sediment. Geol.*, *104*(1–4), 155–173, doi:10.1016/0037-0738(95)00126-3.
Cogné, J. P. (2003), PaleoMac: A Macintosh application for treating paleomagnetic data and making plate reconstructions, *Geochem. Geophys. Geosyst.*, *4*(1), 1007, doi:10.1029/2001GC000227.
Collombat, H., P. Rochette, and D. V. Kent (1993), Detection and correction of inclination shallowing in deep sea sediments using the anisotropy of anhysteretic remanence, *Bull. Soc. Geol. Fr.*, *164*(1), 103–111.
Curray, J. R. (2014), The Bengal depositional system: From rift to orogeny, *Mar. Geol.*, *352*, 59–69, doi:10.1016/j.margeo.2014.02.001.
Curray, J. R., F. J. Emmel,and D. G. Moore (2003), The Bengal Fan: Morphology, geometry, stratigraphy, history and processes, *Mar. Pet. Geol.*, *19*(10), 1191–1223, doi:10.1016/S0264-8172(03)00035-7.
Dade, W. B., and H. E. Huppert (1994), Predicting the geometry of channelized deep-sea turbidites., *Geology*. vol. *22*, 645–648.
Day, R., M. Fuller, and V. A. Schmidt (1977), Hysteresis properties of titanomagnetites: Grain-size and compositional dependence, *Phys. Earth Planet. Inter.*, *13*(4), 260–267, doi:10.1016/0031-9201(77)90108-X.
Dickinson, W. R., and R. F. Butler (1998), Coastal and Baja California paleomagnetism reconsidered., *Geol. Soc. Am. Bull.*, *110*(10), 1268–1280.
Drab, L., A. Hubert-Ferrari, S. Schmidt, P. Martinez, J. Carlut, and M. El Ouahabi (2015), Submarine earthquake history of the Çınarcık segment of the North Anatolian Fault in the Marmara Sea, Turkey, *Bull. Seismol. Soc. Am.*, *105*(2A), 622–645.
Dunlop, D. J. (2002), Theory and application of the Day plot (M rs/M s versus H cr/H c) 1. Theoritical curves and tests using titanomagnetite data, *J. Geophys. Res.*, *107*(B3), 2056, doi:10.1029/2001JB000487.
Enkin, R. J., J. Baker, and P. S. Mustard (2001), *Paleomagnetism of the Upper Cretaceous Nanaimo Group, southwestern Canadian*, Revue canadienne des Sciences de la Terre, *38*(10), 1403–1422. doi:10.1139/cjes-38-10-1403.
Garcés, M., J. M. Parés, and L. Cabrera (1996), Further evidence for inclination shallowing in red beds, *Geophys. Res. Lett.*, *23*(16), 2065–2068.
Griffiths, D. H., R. F. King,A. I. Rees,and A. E. Wright (1960), The remanent magnetism of some recent varved sediments., *Proc. R. Soc. London Ser.* A, *256*(1286), 359–383.
Heslop, D., A. Witt, T. Kleiner, and K. Fabian (2006), The role of magnetostatic interactions in sediment suspensions, *Geophys. J. Int.*, *165*(3), 775–785, doi:10.1111/j.1365-246X.2006.02951.x.
Heslop, D., A. P. Roberts, and R. Hawkins (2014), A statistical simulation of magnetic particle alignment in sediments, *Geophys. J. Int.*, *197*(2), 828–837, doi:10.1093/gji/ggu038.
Jackson, M., S. K. Banerjee, and J. A. Marvin (1991), Detrital remanence, inclination errors, and anhysteretic remanence anisotropy: Quantitative model and experimental results, *Geophys. J.*, *104*(1), 95–103, doi:10.1111/j.1365-246X.1991.tb02496.x.
Jezek, J., S. Gilder, and D. Bilardello (2012), Numerical simulation of inclination shallowing by rolling and slipping of spherical particles, *Comput. Geosci.*, *49*, 270–277, doi:10.1016/j.cageo.2012.06.013.
Katari, K., L. Tauxe, and J. King (2000), A reassessment of post-depositional remanent magnetism: Preliminary experiments with natural sediments, *Earth Planet. Sci. Lett.*, *183*(1–2), 147–160, doi:10.1016/S0012-821X(00)00255-7.
Khan, M. J., N. D. Opdyke,and R. A. K. Tahirkheli (1988), Magnetic stratigraphy of the Siwalik group, Bhittani, Marwat and Khasor ranges, northwestern Pakistan and the timing of neocene tectonics of the Trans Indus, *J. Geophys. Res.*, *93*(10), 11,773–11,790.
Kim, B., and K. P. Kodama (2004), A compaction correction for the paleomagnetism of the Nanaimo Group sedimentary rocks: Implications for the Baja British Columbia hypothesis, *J. Geophys. Res.*, *109, B02102*, doi:10.1029/2003JB002696.
Kneller, B., B. Kneller, W. D. Mccaffrey,and W. D. Mccaffrey (2003), The interpretation of vertical sequences in turbidite beds: The influence of longitudinal flow, *J. Sediment. Res.*, *73*(5), 706–713, doi:10.1306/031103730706.
Kodama, K. P. (1997), Correction to "A successful rock magnetic technique for correcting paleomagnetic inclination shallowing: Case study of the Nacimiento Formation, New Mexico" by K. P. Kodama, *J. Geophys. Res.*, *102*(B4), 7963–7963, doi:10.1029/97JB00752.
Kodama, K. P., and J. M. Davi (1995), A compaction correction for the paleomagnetism of the Cretaceous Pigeon Point Formation of California, *Tectonics*, *14*(5), 1153–1164, doi:10.1029/95TC01648.
Köng, E., S. Zaragosi, J. Schneider, T. Garlan, P. Bachèlery, L. San, C. Seibert, and C. Racine (2016), Untangling the complex origin of turbidite activity on the Calabrian Arc (Ionian Sea) over the last 60 ka, *Mar. Geol.*, *373*, 11–25, doi:10.1016/j.margeo.2015.12.010.
Levi, S., and S. Banerjee (1990), On the origin of inclination shallowing in redeposited sediments, *J. Geophys. Res.*, *95*(B4), 4383–4389, doi:10.1029/JB095iB04p04383.
Lykousis, V., D. Sakellariou, I. Moretti, and H. Kaberi (2007), Late Quaternary basin evolution of the Gulf of Corinth: Sequence stratigraphy, sedimentation, fault-slip and subsidence rates, *Tectonophysics*, *440*(1–4), 29–51, doi:10.1016/j.tecto.2006.11.007.
Middleton, G. V. (1993), Sediment deposition from turbidity currents., *Annu. Rev. Earth Planet. Sci.*, *21*, 89–114.
Moretti, I., V. Lykousis, D. Sakellariou, J. Y. Reynaud, B. Benziane, and A. Prinzhoffer (2004), Sédimentation et vitesse de subsidence dans le golfe de Corinthe: Données acquises grâce aux carottes du Marion Dufresne, *C. R. Geosci.*, *336*(4–5), 291–299, doi:10.1016/j.crte.2003.11.011.
Normark, W. R., D. J. W. Piper,H. Posamentier, C. Pirmez, and S. Migeon (2002), Variability in form and growth of sediment waves on turbidite channel levees, *Mar. Geol.*, *192*(1–3), 23–58, doi:10.1016/S0025-3227(02)00548-0.
Peakall, J., and E. J. Sumner (2015), Submarine channel flow processes and deposits: A process-product perspective, *Geomorphology*, vol. *244*, 95–120:, doi:10.1016/j.geomorph.2015.03.005.
Peakall, J., B. Mccaffrey, and B. E. N. Kneller (2000), A process model for the evolution, morphology, and architecture of sinuous submarine channels, *J. Sediment. Res.*, *70*(3), 434–448, doi:10.1306/2DC4091C-0E47-11D7-8643000102C1865D.
Piguet, B., D. F. McNeill, and P. Kindler (2000), Tectonic rotation and diverse remanence carriers revealed by the paleomagnetism of Eo-Oligocene turbidites from two Ultrahelvetic units (Western Alps, Haute-Savoie, France), *Tectonophysics*, *321*(3), 359–375, doi:10.1016/S0040-1951(00)00071-8.
Quidelleur, X., J. Valet, M. LeGoff, and X. Bouldoire (1995), Field dependence on magnetization of laboratory-redeposited deep-sea sediments: First results, *Earth Planet. Sci. Lett.*, *133*(3-4), 311–325, doi:10.1016/0012-821X(95)00088-T.

Rees, A. I. (1961), The effect of water currents on the magnetic remanence and anisotropy of susceptibility of some sediments. *Geophys. J. Int.*, *5*(3), 235–251.

Shcherbakov, V., and N. Sycheva (2010), On the mechanism of formation of depositional remanent magnetization, *Geochem. Geophys. Geosyst.*, *11*, Q02Z13, doi:10.1029/2009GC002830.

Spassov, S., and J. Valet (2012), Detrital magnetizations from redeposition experiments of different natural sediments, *Earth Planet. Sci. Lett.*, *351-352*, 147–157, doi:10.1016/j.epsl.2012.07.016.

St.-Onge, G., T. Mulder, D. J. W. Piper, C. Hillaire-Marcel, and J. S. Stoner (2004), Earthquake and flood-induced turbidites in the Saguenay Fjord (Québec): A Holocene paleoseismicity record, *Quat. Sci. Rev.*, *23*(3-4), 283–294, doi:10.1016/j.quascirev.2003.03.001.

St.-Onge, G., et al. (2012), Comparison of earthquake-triggered turbidites from the Saguenay (Eastern Canada) and Reloncavi (Chilean margin) Fjords: Implications for paleoseismicity and sedimentology, *Sediment. Geol.*, *243-244*, 89–107, doi:10.1016/j.sedgeo.2011.11.003.

Stoner, J. S., J. E. T. Channell,and C. Hillaire-Marcel (1996), The magnetic signature of rapidly deposited detrital layers from the Deep Labrador Sea: Relationship to North Atlantic Heinrich layers, *Paleoceanography*, *11*(3), 309–325, doi:10.1029/96PA00583.

Tan, X. (2003), Paleomagnetism and magnetic anisotropy of Cretaceous red beds from the Tarim basin, northwest China: Evidence for a rock magnetic cause of anomalously shallow paleomagnetic inclinations from central Asia, *J. Geophys. Res.*, *108*(B2), 2107, doi:10.1029/2001JB001608.

Tan, X., and K. P. Kodama (1998), Compaction-corrected inclinations from southern California Cretaceous marine sedimentary rocks indicate no paleolatitudinal offset for the Peninsular Ranges terrane, *J. Geophys. Res.*, *103*(B11), 27,169–27,192.

Tan, X., K. P. Kodama,and D. Fang (2002), Laboratory depositional and compaction-caused inclination errors carried by haematite and their implications in identifying inclination error of natural remanence in red beds, *Geophys. J. Int.*, *151*(2), 475–486, doi:10.1046/j.1365-246X.2002.01794.x.

Tauxe, L. (1993), Sedimentary records of relative paleointensity of the geomagnetic field: Theory and practice, *Rev. Geophys.*, *31(3)*, 319–354, doi:10.1029/93RG01771.

Tauxe, L., and D. V. Kent (1984), Properties of a detrital remanence carried by haematite from study of modern river deposits and laboratory redeposition experiments, *Geophys. J. R. Astron. Soc.*, *77*, 543–561.

Tauxe, L., J. L. Steindorf, and A. Harris (2006), Depositional remanent magnetization: Toward an improved theoretical and experimental foundation, *Earth Planet. Sci. Lett.*, *244*(3-4), 515–529, doi:10.1016/j.epsl.2006.02.003.

Toucanne, S., S. Zaragosi, J. Bourillet, B. Dennielou, S. J. Jorry,G. Jouet, and M. Cremer (2012), Archimer Armorican margin (Bay of Biscay, western European margin), *Mar. Geol.*, *303–306*, 137–153.

Valet, J. P., E. Moreno, F. Bassinot, L. Johannes, F. Dewilde, T. Bastos, A. Lefort, and Venec-M. T. Peyre (2011), Isolating climatic and paleomagnetic imbricated signals in two marine cores using principal component analysis, *Geochem. Geophys. Geosyst.*, *12*, Q08012, doi:10.1029/2011GC003697.

Valet, J. P., F. Bassinot, A. Bouilloux, D. Bourlès, S. Nomade, V. Guillou, F. Lopes, N. Thouveny, and F. Dewilde (2014), Geomagnetic, cosmogenic and climatic changes across the last geomagnetic reversal from Equatorial Indian Ocean sediments, *Earth Planet. Sci. Lett.*, *397*, 67–79, doi:10.1016/j.epsl.2014.03.053.